Fractals, Vol. 23, No. 1 (2015) 1540010 (11 pages)

DOI: 10.1142/S0218348X15400101

World Scientific
www.worldscientific.com

BI-PHASE BOX COUNTING: AN IMPROVED METHOD FOR FRACTAL ANALYSIS OF BINARY IMAGES

E. PERFECT* and B. DONNELLY
Department of Earth and Planetary Sciences
University of Tennessee Knoxville
Knoxville, TN 37996, USA
**eperfect@utk.edu*

Received July 15, 2014
Accepted September 20, 2014
Published February 25, 2015

Abstract

Many natural systems are irregular and/or fragmented, and have been interpreted to be fractal. An important parameter needed for modeling such systems is the fractal dimension, D. This parameter is often estimated from binary images using the box-counting method. However, it is not always apparent which fractal model is the most appropriate. This has led some researchers to report different D values for different phases of an analyzed image, which is mathematically untenable. This paper introduces a new method for discriminating between mass fractal, pore fractal, and Euclidean scaling in images that display apparent two-phase fractal behavior when analyzed using the traditional method. The new method, coined "bi-phase box counting", involves box-counting the selected phase and its complement, fitting both datasets conjointly to fractal and/or Euclidean scaling relations, and examining the errors from the resulting regression analyses. Use of the proposed technique was demonstrated on binary images of deterministic and stochastic fractals with known D values. Traditional box counting was unable to differentiate between the fractal and Euclidean phases in these images. In contrast, bi-phase box counting unmistakably identified the fractal phase and correctly estimated

*Corresponding author.

its D value. The new method was also applied to three binary images of soil thin sections. The results indicated that two of the soils were pore-fractals, while the other was a mass fractal. This outcome contrasted with the traditional box counting method which suggested that all three soils were mass fractals. Reclassification has important implications for modeling soil structure since different fractal models have different scaling relations. Overall, bi-phase box counting represents an improvement over the traditional method. It can identify the fractal phase and it provides statistical justification for this choice.

Keywords: Sierpinski Gasket; Percolation Cluster; Soil Thin Section; Segmented Regression; Mass Fractal; Pore Fractal.

1. INTRODUCTION

Many natural systems are irregular and/or fragmented, and have been interpreted to be fractal; that is, they exhibit statistical self-similarity or self-affinity over wide ranges of spatial and/or temporal scales.[1] This recognition has resulted in the development of many theoretical models for predicting the scaling behavior of natural systems. However, the fractal parameters for a particular system must first be determined before these models can be applied.[2]

The most important and well-known fractal parameter needed for modeling is the "fractal dimension". The fractal dimension provides a scale-invariant measure of the space or time-filling capacity of a property or process.[3] It is commonly estimated using the box-counting method.[1,4] According to this method, boxes of size x are superimposed upon a binary image of a complex structure. A choice is made as to which phase (black or white) is to be characterized, and the number of boxes, N, containing that phase is counted. The size of the boxes is then reduced and N is measured again. This process is repeated until the boxes approach the size of the pixels or voxels that make up the image. If the selected phase is fractal, the following power law relation should hold[1,4]:

$$N \propto x^{-D}, \tag{1}$$

where D is the box counting fractal dimension.

In a physical system, such as a porous medium, the different phases of a binary image represent solids and voids. Depending on which phase Eq. (1) is applied to, the system is then referred to as a pore or mass fractal.[5]

Fitting Eq. (1) to a given phase imposes certain, often unstated conditions, on the nature of the scaling of the complementary phase. For fractal systems, the complement of the counted fractal phase is Euclidean[5,6] and should scale as:

$$N \propto x^{-E}, \tag{2}$$

where E (=1, 2, or 3) is the Euclidean dimension. It is also possible when box counting that the system is Euclidean, in which case both phases will scale according to Eq. (2).

With natural systems it is not always apparent which box counting model (mass, pore, or Euclidean) is most appropriate. Thus, it is tempting to fit Eq. (1) separately to box counting data for both phases in an effort to identify the fractal phase based on goodness-of-fit statistics. Unfortunately, Eq. (1) usually fits both phases equally well in terms of coefficients of determination (R^2). Moreover, both estimates of D can be significantly different from each other as well as significantly less than E. While this is not mathematically tenable, it has led some researchers to report separate D values for both phases of an analyzed binary image.[2,7]

The separate application of Eq. (1) to both phases of binary image presents a mathematical problem that can lead to misleading conclusions. If one phase is fractal, then the other phase should exhibit Euclidean scaling.[5,6] Previous attempts to determine a means of identifying the true fractal phase in natural systems have produced mixed results.[5,8] From a practical perspective, identifying which phase is fractal has major implications for the development and parameterization of scale-invariant models for natural systems.

This paper introduces a new method ("bi-phase box counting") for discriminating between mass fractal, pore fractal, and Euclidean scaling in natural systems that display apparent two-phase fractal behavior when analyzed using the traditional box counting technique. The proposed method involves box-counting a given phase and its complement, fitting both datasets conjointly to appropriate fractal

and/or Euclidean scaling relations, and examining the errors from the resulting regression analyses. The method is tested on two known fractals (the Sierpinski gasket and Bernoulli percolation cluster) and then applied to binary images of three soil thin sections (STSs).

2. TRADITIONAL AND BI-PHASE BOX COUNTING

In traditional box counting analysis of binary images, Eq. (1) is linearized by log–log transformation and fitted to the black and white phases separately, i.e.

$$\log N_b = \log k_b - D_b \log x, \tag{3a}$$

$$\log N_w = \log k_w - D_w \log x, \tag{3b}$$

where the subscripts b and w denote the number of boxes and parameters for the black and white phases, respectively.

As discussed in the preceding section it is theoretically impossible for both phases in a binary image to be fractal. However, Eq. (3) frequently fits both phases equally well yielding two different estimates of $D < E$ so that it is impossible to decide which phase is the true fractal phase using this approach. This is because Eq. (3) fails to take into account the scaling behavior of the complementary phase.

In the case of bi-phase box counting both phases are fitted conjointly using the following equations:

$$\begin{aligned}\log N_b &= \log k_b - D \log x \wedge \log N_w \\ &= \log k_w - 2 \log x,\end{aligned} \tag{4a}$$

$$\begin{aligned}\log N_w &= \log k_w - D \log x \wedge \log N_b \\ &= \log k_b - 2 \log x,\end{aligned} \tag{4b}$$

$$\begin{aligned}\log N_w &= \log k_w - 2 \log x \wedge \log N_b \\ &= \log k_b - 2 \log x,\end{aligned} \tag{4c}$$

where $\wedge$ is the logical "AND" operator. Conjoint fitting means that both expressions are fitted to the box counting data simultaneously by minimizing the residuals using the method of least squares. In statistics, this process is known as segmented or piecewise regression.[9]

Equations (4a) and (4b) only allow one of the phases to be fractal, since the complementary phase is forced to follow Euclidean power law scaling. In Eq. (4a) the black phase is fractal and the white phase is Euclidean, while in Eq. (4b) the white phase is fractal and the black phase is Euclidean. In contrast, neither phase is fractal in Eq. (4c) since both phases follow Euclidean power law scaling. Thus, fitting Eq. (4) to box counting results for both phases enables a decision to be made as to which model is most appropriate based on best fit statistics such as the coefficient of determination (R^2) and residual sum of squares (RSS). The equation producing the highest R^2 and/or lowest RSS values is selected as the most appropriate model, i.e. pore fractal [Eq. (4a) when the black phase represents pores], mass fractal [Eq. (4b) when the white phase represents solids], or Euclidean [Eq. (4c) when both the black and white phases are Euclidean].

3. MATERIALS AND METHODS

Five binary images were analyzed in this study: two known fractals (Fig. 1) and three thresholded STSs with different structural characteristics (Fig. 2). Relevant physical characteristics of the images determined using ImageJ[10] are given in Table 1. Figure 1a is a Sierpinski gasket provided with the BENOIT™ fractal analysis software package.[11] The theoretical D value for this deterministic fractal is 1.584... (Mandelbrot[3]). Figure 1b is a Bernoulli percolation cluster from Sukop *et al.*[12] The theoretical D value of this stochastic fractal is 1.895...[12] The soil thin section images were originally published by Zhou *et al.*[13,14] and details pertaining to the soil type, sampling procedure, thin section preparation, and image acquisition can be found in those references. The original 256-bit grayscale images from Zhou *et al.*[13,14] were converted to binary using the mean value thresholding method.

Box counting was performed with the BENOIT™ program. In this program, binary bitmap images are analyzed by counting the "white phase" of an image. To facilitate box counting of both phases, inverted images of the five binary images were created. Each of the five binary images as well as their inverted complements was then analyzed with the BENOIT™ software. Hereafter, when discussing box counting results for the "black phase", it should be understood that we are referring to results obtained from the analyses of the inverted images.

The BENOIT™ software includes a limited number of user-defined parameters for the box-counting analysis. The maximum cutoff point, or the side length of the largest counted box, can be set manually, but the default value of 25% of the image width was used in this study. The coefficient

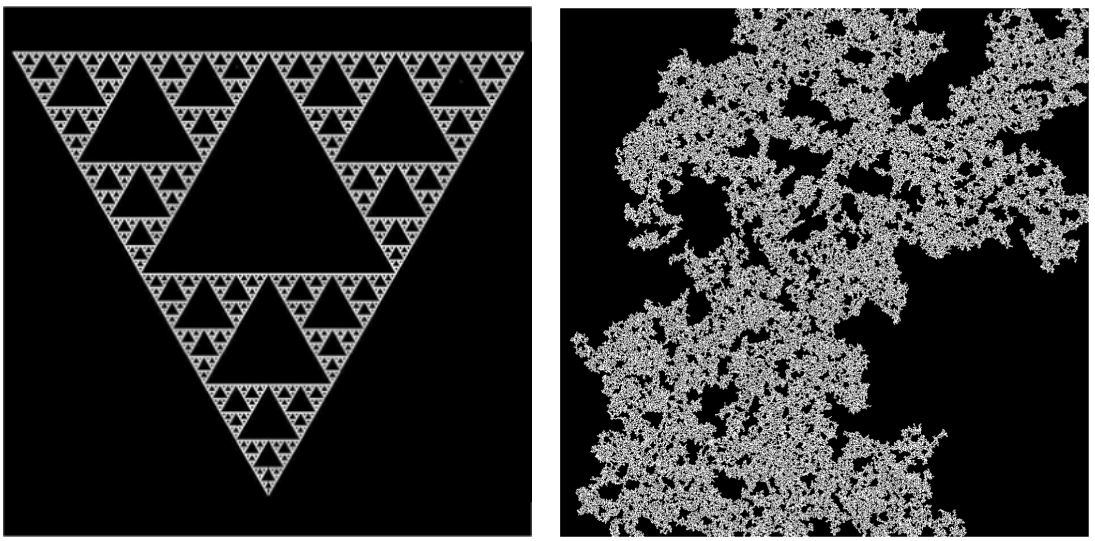

(a) **(b)**

Fig. 1 **(a)** Sierpinski gasket ($D = 1.584\ldots$) and **(b)** Bernoulli percolation cluster ($D = 1.895\ldots$) images with the fractal phase shown in white and the Euclidean phase in black.

of box size decrease, or the scaling factor of the grid, is also user-defined and was set to the lowest value (1.1) so as to produce the largest number of measurements. Benoit also rotates the grid and uses the minimum number of occupied boxes in a 90° rotation. This rotation is the last controllable parameter and was it set to an increment of 5°.

The log–log transformed box counting results were exported to the SAS statistical analysis program,[9] and Eqs. (3a) and (3b) were fitted to the black and white phases separately using linear regression. These analyses represent the traditional box counting approach. Additionally, biphase box counting analyses were performed by fitting Eqs. (4a), (4b), and (4c) to the log–log transformed box counting data using segmented linear regression (Levenberg–Marquardt algorithm) in SAS. Equation (4a) assumes the black phase is fractal and the white phase Euclidean, Eq. (4b) assumes the converse, while Eq. (4c) assumes both phases

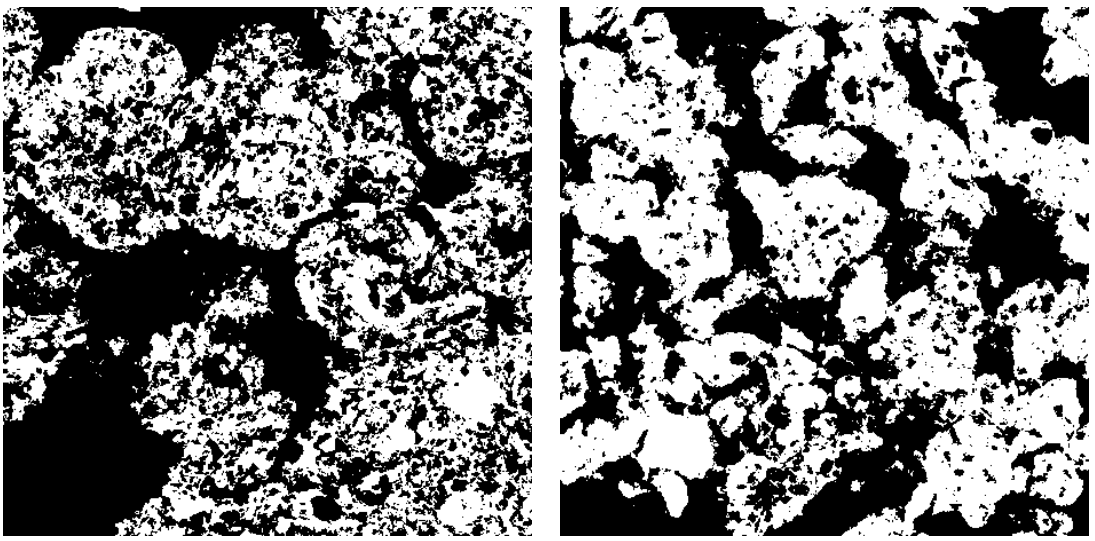

(a) **(b)**

Fig. 2 Binary STS images from Ref. 14 with the solid phase shown in white and the pore phase in black: **(a)** STS #1, **(b)** STS #2 and **(c)** STS #3.

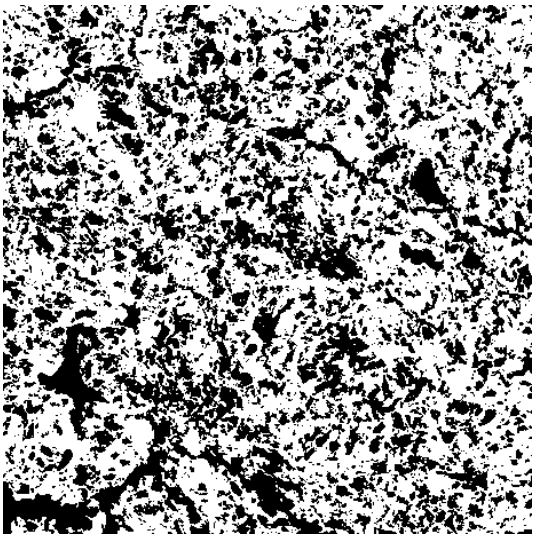

(c)

Fig. 2 (*Continued*)

Table 1 Properties of the Images Analyzed: L is Maximum Side Length, and ϕ_b and ϕ_w are the Fractions of Black and White Pixels, respectively.

Image	L (Pixels)	ϕ_b	ϕ_w
1A	320	0.86	0.14
1B	1024	0.73	0.27
2A	1024	0.59	0.41
2B	1024	0.47	0.53
2C	1024	0.40	0.60

are Euclidean. Thus, the regression equation with the highest R^2 and/or lowest RSS values can be used to identify the best model. Unless otherwise noted, statistical significance was always assessed at the 0.05 probability level (i.e. 95% confidence level).

4. RESULTS AND DISCUSSION

The results of the separate (traditional) box counting analyses of the black and white phases in the Sierpinski gasket image (Fig. 1a) are shown in Fig. 3. Equation (3) fitted both phases equally well as can be seen from the goodness-of-fit statistics presented in Table 2. The R^2 values were equal, but the RSS value for the white phase was slightly lower than that for the black phase indicating a marginally better fit for Eq. (3a) as compared to Eq. (3b), and suggesting the white phase is the true fractal phase (Table 4). However, both estimates

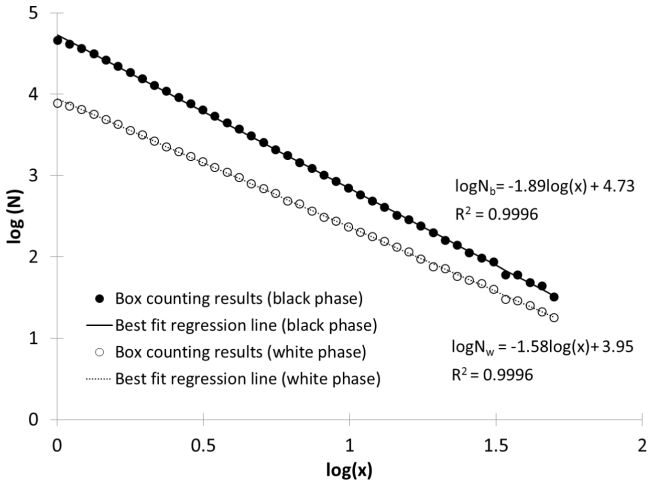

Fig. 3 Results of box counting analyses performed on the Sierpinski gasket image in Fig. 1a using the traditional method treating the black and white phases separately, Eq. (3).

Table 2 Summary of Best Fit Parameters and Regression Statistics[a] from the Separate Fitting of Eq. (3) to Box Counting Results for the Black and White Phases of Known Fractals (Fig. 1) and STSs (Fig. 2).

Image	Fractal Phase	$\log k\,(S_E)$	$D\,(S_E)$	R^2	RSS
Fig. 1a	black	4.730 (0.006)	1.889 (0.006)	0.9996	0.017
	white	3.948 (0.005)	1.582 (0.005)	0.9996	0.011
Fig. 1b	black	5.944 (0.017)	1.924 (0.012)	0.9992	0.034
	white	5.567 (0.018)	1.787 (0.005)	0.9990	0.037
Fig. 2a	black	5.816 (0.010)	1.860 (0.007)	0.9992	0.079
	white	5.664 (0.009)	1.800 (0.006)	0.9993	0.062
Fig. 2b	black	5.685 (0.009)	1.797 (0.007)	0.9992	0.076
	white	5.720 (0.006)	1.825 (0.004)	0.9997	0.033
Fig. 2c	black	5.697 (0.016)	1.794 (0.011)	0.9977	0.214
	white	5.842 (0.010)	1.874 (0.007)	0.9992	0.078

[a]S_E = approximate standard error, R^2 = coefficient of determination, RSS = residual sum of squares.

of the fractal dimension, D, were significantly less than two (E) and significantly different from each other (Table 2). Thus, if one did not know *a priori* which is the true fractal phase it would be very difficult to decide which D value is correct and which one is fallacious. The theoretical fractal dimension of the Sierpinski gasket is $D = 1.584\ldots$[3] Thus, in this case, it is clear that the white phase is the true fractal phase case since the regression estimate of D (= 1.582) for this phase (Table 4) was within a fraction of a percent of the true value.

The apparent "dual-phase" fractal behavior illustrated in Fig. 3, with two different fractal dimensions, is in direct conflict with accepted fractal theory and highlights the need for an alternative method for determining the most appropriate fractal model. The results of box counting both phases of the Sierpinski gasket image concomitantly based on the proposed bi-phase method are shown in Fig. 4. Equation (4a) (which assumes the black phase is fractal and the white phase Euclidean), (4b) (which assumes the black phase is Euclidean and the white phase fractal), and (4c) (which assumes the black and white phases are both Euclidean), were fitted to the box counting data using segmented linear regression. These regression analyses are summarized in Table 3, and the resultant predicted linear relationships are included in Figs. 4a–4c.

From visual inspection of Fig. 4 it can be clearly seen that Eq. (4b) provides a much better fit to the combined data than either Eq. (4a) or Eq. (4c), thereby correctly identifying the white phase as fractal and the black phase as Euclidean. The goodness-of-fit statistics and parameter estimates presented in Table 3 confirm this conclusion. The RSS error associated with fitting Eq. (4b) to the box counting results was over an order of magnitude lower than that associated with fitting Eq. (4a). Most importantly, the D value estimated by Eq. (4a) was erroneous (Table 3), whereas the

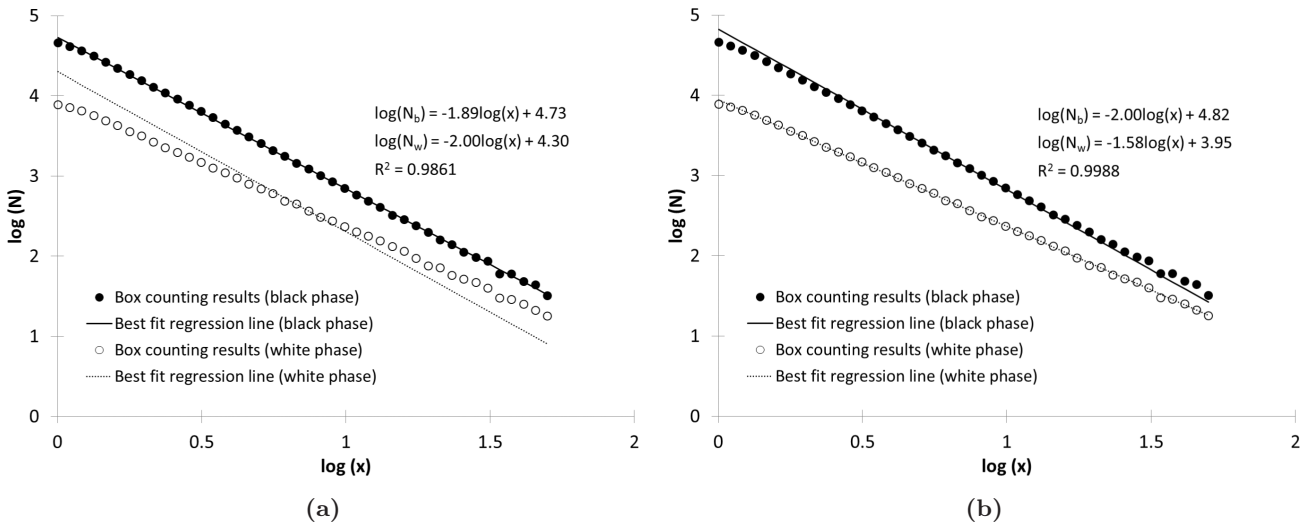

Fig. 4 Results of bi-phase box counting analyses performed on the Sierpinski gasket image in Fig. 1a with: **(a)** the black phase assumed to be fractal and the white phase Euclidean, Eq. (4a), **(b)** the black phase assumed to be Euclidean and the white phase fractal, Eq. (4b) and **(c)** both phases assumed to be Euclidean, Eq. (4c).

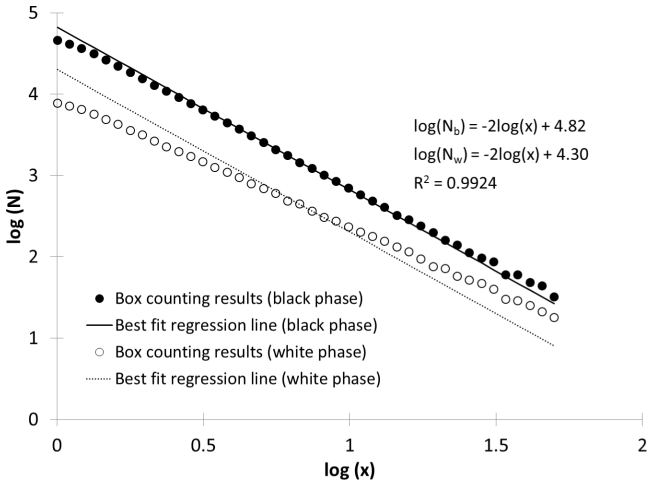

(c)

Fig. 4 (*Continued*)

D value estimated by fitting Eq. (4b) to the box counting data ($D = 1.582$) was within a fraction of a percent of the known fractal dimension for the Sierpinski carpet of $D = 1.584$.

Separate and conjoint box counting analyses were also performed on the Bernoulli percolation cluster illustrated in Fig. 1b. The graphical results were quite similar to those for the Sierpinski gasket and are not illustrated. However, the statistical results of fitting Eqs. (3) and (4) to the box counting data have been included in Tables 2 and 3, respectively. As was the case for the Sierpinski carpet, the separate (traditional) box counting analyses using Eq. (3) erroneously indicated that both phases were fractal. The resulting estimates of D were both significantly less than two (E); they were also significantly different from each other (Table 2). Furthermore, the goodness-of-fit statistics in Table 2, incorrectly identified Eq. (3a) fitted to the black phase as the most appropriate fractal model. In contrast, the bi-phase box counting results correctly identified Eq. (4b) fitted to the white phase as the most appropriate fractal model (see Tables 3 and 4). The resulting estimate of D ($= 1.787\ldots$) was within

Table 3 Summary of Best Fit Parameters and Regression Statistics[a] from the Conjoint Fitting of Eq. (4) to Box Counting Results for the Black and White Phases of Known Fractals (Fig. 1) and STSs (Fig. 2).

Image	Equation	Fractal Phase	$\log k_b\,(S_E)$	$\log k_w\,(S_E)$	$D/E\,(S_E)$	R^2	RSS
Fig. 1a	4a	black	4.730 (0.046)	4.303 (0.024)	1.889 (0.047)	0.9861	1.874
	4b	white	3.948 (0.013)	4.824 (0.007)	1.582 (0.014)	0.9988	0.157
	4c	neither	4.824 (0.024)	4.303 (0.024)	2.000 (0.000)	0.9924	2.004
Fig. 1b	4a	black	5.944 (0.050)	5.825 (0.026)	1.927 (0.035)	0.9960	0.592
	4b	white	6.032 (0.021)	5.567 (0.024)	1.787 (0.017)	0.9988	0.132
	4c	neither	6.032 (0.027)	5.825 (0.027)	2.000 (0.000)	0.9977	0.653
Fig. 2a	4a	black	5.816 (0.028)	5.906 (0.014)	1.860 (0.020)	0.9965	1.316
	4b	white	5.664 (0.020)	5.985 (0.010)	1.800 (0.015)	0.9980	0.716
	4c	neither	5.906 (0.017)	5.985 (0.017)	2.000 (0.000)	0.9990	1.892
Fig. 2b	4a	black	5.685 (0.024)	5.932 (0.012)	1.797 (0.017)	0.9973	1.011
	4b	white	5.720 (0.028)	5.931 (0.014)	1.825 (0.020)	0.9965	1.323
	4c	neither	5.932 (0.018)	5.931 (0.018)	2.000 (0.000)	0.9994	2.225
Fig. 2c	4a	black	5.697 (0.021)	5.994 (0.011)	1.794 (0.015)	0.9974	0.761
	4b	white	5.842 (0.030)	5.946 (0.015)	1.874 (0.021)	0.9967	1.542
	4c	neither	5.994 (0.017)	5.946 (0.017)	2.000 (0.000)	0.9980	2.011

[a] S_E = approximate standard error, R^2 = coefficient of determination, RSS = residual sum of squares.

Table 4 Inferred Fractal Phases/Models, and their Fractal Dimensions, for two Known Fractals (Fig. 1) and Three STSs (Fig. 2).

Image	Inferred Fractal Phase from Eq. (3)	D	Inferred Fractal Phase from Eq. (4)	D
Fig. 1a	white	1.582	white	1.582
Fig. 1b	black	1.924	white	1.787
Fig. 2a	white (mass)	1.800	white (mass)	1.800
Fig. 2b	white (mass)	1.825	black (pore)	1.797
Fig. 2c	white (mass)	1.874	black (pore)	1.794

6% of the theoretical value for the Bernoulli percolation cluster ($D = 1.895\ldots$), although the difference between the two values was statistically significant. The less accurate estimation of D in this case, as compared to that for the Sierpinski gasket, is likely due to the fact that Bernoulli percolation cluster is a stochastic fractal whereas the Sierpinski gasket is a deterministic fractal. In the former, $N(x)$ varies slightly from one realization to another, while in the later $N(x)$ is always the same. Since Fig. 1b represents a single realization of the Bernoulli percolation cluster its D value can be expected to deviate slightly from the theoretical value expected from averaging results from multiple realizations.

Having successfully tested the proposed bi-phase box counting method on two known fractals, we then applied it to three binary STS images in which the true nature of the fractal scaling is unknown. As was the case with the known fractals, separate fits of Eq. (3) to each phase produced dual estimates of D that were significantly less than three and significantly different from each other (Table 2). The D values ranged from 1.794 to 1.860 for the black (pore) phase and from 1.800 to 1.874 for the white (solid) phase. The associated goodness-of-fit statistics for Eq. (3) applied to the different phases in each thin section image were not very different (Table 2). However, based on the criteria of highest R^2 and/or lowest RSS values, the traditional box counting method identified the white (solid) phase as the best fractal model for each image; i.e. all three STS images were classified as mass fractals based on this method (Table 4).

The results of the bi-phase box counting analyses of the three soil thin section images are summarized in Table 3. In contrast to the separate (traditional) method of fitting Eq. (3), Eq. (4) fits the data for the black and white phases at the same time. While the R^2 values for Eqs. (4a), (4b), and (4c) fitted to the STS images were all >0.99, the RSS error values were quite different and allow for a clear identification of the best fitted model. Based on the criteria of lowest RSS values, the bi-phase method classified STS#1 as a mass fractal, i.e. Eq. (4b), and STS#2 and STS#3 as pore fractals, Eq. (4a) (Table 4). This result is quite different from that obtained using Eq. (3), which identified all three thin sections as mass fractals. Correct identification of the most appropriate fractal model is critical when simulating soil structure, since the physiochemical properties of pore fractals are very different from those of mass fractals.

Measured versus predicted box counting results for the three binary STS images are shown in Fig. 5. The predicted values were computed from the best fit fractal models, i.e. Eq. (4b) in the case of STS#1 and Eq. (4a) for STS#2 and STS#3. The fits for STS#1 and STS#3 were quite good overall, with only relatively minor deviations from the 1:1 relationship at very small or very large box sizes. The worst fit occurred with STS#2 (Fig. 2b). In this case, the pore fractal model systematically over and under predicted the numbers of boxes containing pores (black pixels) at large and small box sizes, respectively (Fig. 5b). Despite being the best fitting model for this STS, the poor performance of Eq. (4a) is reflected in its relatively high RSS and low R^2 values compared to the corresponding values for the other images (Table 3). The reason why bi-phase box counting performed poorly in this case is unclear, but it may be related in some way to the fact that the areal fractions of black (pore) and white (solid) pixels were approximately equal in this image, whereas there was a pronounced dominant phase in all of the other images (Table 1).

It is interesting to note that the choice of fractal model appears to depend upon the areal fractions of black and white pixels in the images analyzed (compare Tables 1 and 4). Images with high proportions of black pixels were best described by a mass fractal model, while images with high proportions of white pixels were best described by a pore fractal model. The image with approximately equal fractions of black and white pixels was not well described by either model.

From Table 4, it is clear that all three STS images have very similar fractal dimensions ($D \sim 1.79-1.80$), despite the application of different fractal models and obvious visual differences in their pore space geometry (Fig. 2). This observation, adds much credence to the argument that additional

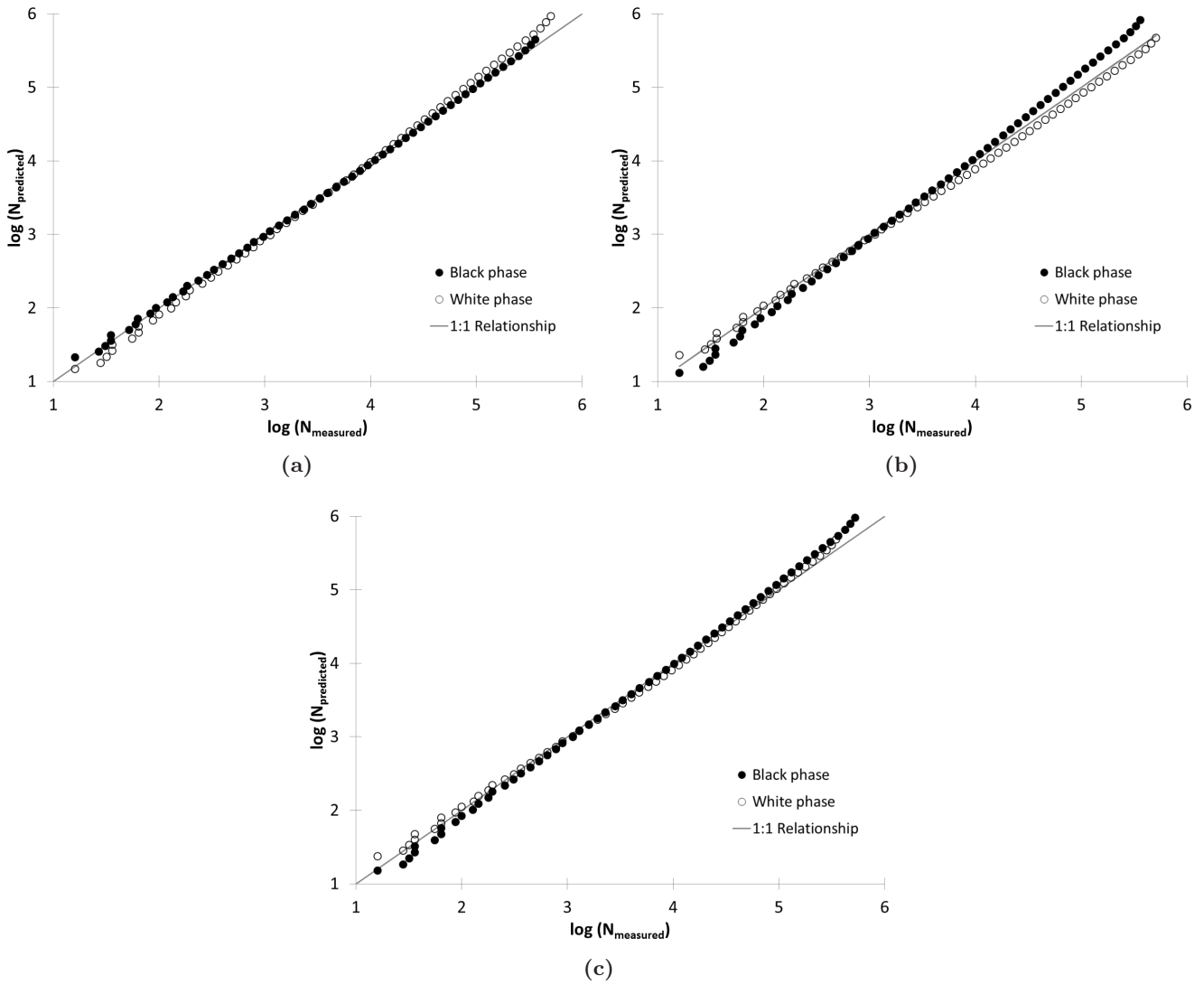

Fig. 5 Measured versus predicted (based on the bi-phase model with the highest R^2 and lowest RSS values) box counting results for the three binary STS images in Fig. 2: **(a)** STS #1, **(b)** STS #2 and **(c)** STS #3.

parameters, such as lacunarity[15] and succolarity,[16] are needed to provide a more thorough quantitative characterization of soil structure using fractal box counting analysis.

Obviously, more studies applying the bi-phase approach to box counting analyses of thin section images will be needed to establish a dominant fractal model for soils. A search of the soils literature in the Science Citation Index[17] using the key words "mass fractal" and "pore fractal" resulted in 6.5 times as many citations for mass fractals as for pore fractals. This suggests that soils are currently primarily viewed as mass fractals. However, the fact that pore fractal scaling was identified as the best model describing soil structure for 2/3 of the thin sections analyzed in this study suggests that the use of pore fractal models for predicting soil properties and processes should be reconsidered.

The STS images were produced by thresholding original grayscale images. Tarquis *et al.*[18] have shown that the choice of thresholding algorithm can strongly influence the estimation of the fractal dimension from such binarized images. In this study, the mean intensity value was used to threshold all three STS images, and so our conclusions regarding the most appropriate fractal models hold for this particular approach. Other thresholding algorithms, however, may result in different goodness-of-fit statistics, and thus different conclusions regarding the most appropriate fractal model. Therefore, additional research on the sensitivity of the proposed bi-phase box counting method

to the choice of thresholding algorithm seems to be warranted in the case of binarized grayscale images.

Box counting has also been applied to the so-called pore-solid fractal (PSF) model.[2,19] In the PSF model, the pore–solid interface is fractal, while box counting the black and white phases, separately results in nonlinear log–log scaling relations that require additional fitting parameters. Since the interfaces of both mass and pore fractals are also fractal,[20] it is not possible to use the bi-phase method proposed here to discriminate between the PSF model and regular fractal or Euclidean models. The problem is further complicated by the fact that generation of an actual PSF model requires a decision to be made as to how to apportion the generator phase between the pores and solids at the terminal (finite) iteration level. As a result, it is not possible to cleanly test the bi-phase box counting method on images of known PSFs as was done in the present study with known fractals. Further work will be required to address this topic.

5. CONCLUSIONS

It has been shown that the traditional box-counting method can produce results which suggest that both phases of a binary image are fractal; i.e. each phase produces a linear relationship on a log–log plot of the number of occupied boxes versus box side length, with both estimated fractal dimensions being statistically different from the Euclidean dimension and statistically different from each other. According to accepted fractal theory such an outcome is not mathematically tenable.

In order to address this issue, an improved box counting technique, coined "bi-phase box counting", has been developed to assist in identifying the most appropriate fractal model for describing binary images of natural fractal systems. This method takes the results from box-counting analyses of a given phase in an image and its complement and simultaneously fits two models (one for fractal scaling and the other for Euclidean scaling) to these data. In essence, it combines box-counting information from both phases of an image and provides goodness-of-fit statistics that facilitate a clear cut decision to be made regarding the most appropriate fractal scaling model.

Use of the proposed technique was demonstrated on binary images, example deterministic and stochastic fractals, i.e. the Sierpinski gasket and Bernoulli percolation cluster, respectively. Traditional box counting analyses were unable to clearly differentiate between the known fractal and Euclidean phases in these images. In contrast, bi-phase box counting unmistakably identified the true fractal phase and accurately estimated their fractal dimensions (to within $\leq 6\%$ of the theoretical values).

The improved method was then applied to three binary images of soil thin sections. The results indicated that the most porous soil ($\phi_b > 0.5$) was best classified as a mass fractal, while the least porous soils ($\phi_b \leq 0.5$) were best classified as pore fractals. This outcome contrasted with the results of traditional box counting analyses which suggested that all three soils are best classified as mass fractals. Identification of the most appropriate fractal scaling relationship is critical for the development of accurate models for simulating soil structure.

Overall, bi-phase box counting represents an improvement over the traditional method. It can assist in the determination of the true fractal phase in binary images of natural systems and it provides statistical justification for this choice. Out of the five images considered in this study, 3/5 were reclassified based on the results of the bi-phase box counting method as compared to the results obtained using the traditional method. Further research is needed to investigate the method's sensitivity to thresholding of grayscale images and its possible applicability to PSF models.

REFERENCES

1. D. L. Turcotte, *Fractals and Chaos in Geology and Geophysics*, 2nd edn. (Cambridge University Press, New York, NY, USA, 1997), p. 398.
2. A. Dathe and M. Thullner, The relationship between fractal properties of solid matrix and pore space in porous media, *Geoderma* **129** (2005) 279–290.
3. B. B. Mandelbrot, *The Fractal Geometry of Nature* (W. H. Freeman, San Francisco, USA), p. 468.
4. R. Lopes and N. Betrouni, Fractal and multifractal analysis: A review, *Med. Image Anal.* **13** (2009) 634–649.
5. J. W. Crawford and N. Matsui, Heterogeneity of the pore and solid volume of soil: Distinguishing a fractal space from its non-fractal complement, *Geoderma* **73** (1996) 183–195.
6. H. Zhou, E. Perfect, B. Li and Y. Lu, Comments on "On the physical properties of apparent two-phase fractal porous media", *Vadose Zone J.* **9** (2010) 192–193.

7. B. Yu, J. Cai and M. Zou, On the physical properties of apparent two-phase fractal porous media, *Vadose Zone J.* **8** (2009) 177–186.
8. N. Bird, M. C. Díaz, A. Saa and A. M. Tarquis, Fractal and multifractal analysis of pore-scale images of soil, *J. Hydrol.* **322** (2006) 211–219.
9. SAS, 2014. SAS/STAT® software, version 9.4, SAS Institute Inc. Cary, NC.
10. C. A. Schneider, W. S. Rasband and K. W. Eliceiri, NIH Image to ImageJ: 25 years of image analysis, *Nat. Methods* **9** (2012) 671–675.
11. TruSoft International Inc. 1999. BENOIT™ Version 1.31. St. Petersburg, FL. Computer Software.
12. M. C. Sukop, G.-J. van Dijk, E. Perfect and W. K. P. van Loon, Percolation thresholds in 2-dimensional prefractal models of porous media, *Transp. Porous Media* **48** (2002) 187–208.
13. H. Zhou, E. Perfect, B. G. Li and Y. Z. Lu, Effects of bit depth on the multifractal analysis of grayscale images, *Fractals* **18** (2010) 127–138.
14. H. Zhou, E. Perfect, Y. Z. Lu, B. G. Li and X. H. Peng, Multifractal analyses of grayscale and binary soil thin section images, *Fractals* **19** (2011) 299–309.
15. J.-W. Kim, E. Perfect and H. Choi, Anomalous diffusion in two-dimensional Euclidean and prefractal geometrical models of heterogeneous porous media, *Water Resour. Res.* **43** (2007) W01405, doi:101029/2006WR004951.
16. R. H. C. de Melo and A. Conci, How succolarity could be used as another fractal measure in image analysis, *Telecommun. Syst.* **52** (2013) 1643–1655.
17. T. Reuters, Web of Science™, Science Citation Index Expanded, accessed on 18 September 2014.
18. A. M. Tarquis, R. J. Heck, J. B. Grau, J. Fabregat, M. E. Sanchez and J. M. Antón, Influence of thresholding in mass and entropy dimension of 3D soil images, *Nonlin. Processes Geophys.* **15** (2008) 881–891.
19. E. Perrier, N. Bird and M. Rieu, Generalizing the fractal model of soil structure: The pore–solid fractal approach, *Geoderma* **88** (1999) 137–164.
20. J. C. Russ, *Fractal Surfaces* (Plenum Press, New York, NY, USA), p. 309.